

## **Pseudo-acoustic wavefield propagation for anisotropic media**

Ben D. Wards, Gary F. Margrave, and Michael P. Lamoureux

### **ABSTRACT**

Reverse-time migration (RTM) is a powerful migration method provided that an accurate velocity model can be constructed. The full elastic wave equation is computationally expensive for modelling and migration. As a result it is preferred to propagate each body wave mode separately with approximate equations instead of propagating with the full elastic wave equation. In isotropic homogeneous media pressure waves satisfy an acoustic wave equation. In heterogeneous isotropic media this wave equation although not strictly valid can be used to approximate propagation of single body wave modes. This acoustic wave equation propagates with the correct phase velocity and ignores mode conversions. For anisotropic media the same procedure can be used to propagate quasi-P and quasi-S waves. The resulting equation is called a pseudo-acoustic wave equation. This equation contains generalizations of partial derivatives called pseudo-differential operators.

### **INTRODUCTION**

Multi-component seismic data is a record of all three displacement components of the seismic wavefield. However, more expensive and sophisticated processing flows are required to leverage this data for improved hydrocarbon detection. The speed of propagation in anisotropic media is sensitive to the direction of propagation. The shear waves are more sensitive to anisotropy than the pressure waves. Tilted Transverse anisotropy (TTI) is a model of anisotropy that reasonably approximates many rocks. The mathematical simplification of the equations of motion provide tractable mathematics for numerical computation while also providing a reasonably accurate model of the physics. TTI reverse-time migration is an accurate method of imaging seismic data provided an accurate velocity model can be constructed.

Many researchers have published results detailing two-way modelling and migration using pseudo-acoustic wavefield propagators. Alkhalifah (2000) derived a pseudo-acoustic wave equation from the coupled dispersion relation for pressure (P) and vertical shear (SV) waves. However, it generates SV-wave artifacts in the solution process. Grechka et al. (2004) explained that the shear wave artifacts arise from setting the vertical shear-wave velocity to zero. While the horizontal shear-wave velocity is non zero as a result of the anisotropy. The shear-wave artifacts give rise to instabilities. There have been many suggestions to stabilize and reduce the shear-wave artifacts. For example, if the vertical shear wave velocity is not set to zero but instead is a given a finite value then instabilities arising from a variable tilt angle can be eliminated. However, this increases the size of the shear-wave artifacts. To reduce the shear-wave artifacts the shear-wave velocity can be solved to reduce reflections and transmissions of P-wave energy into SV-energy (Tsvankin, 2001). To eliminate the formation of S-waves at the source requires injecting the wavelet into an isotropic layer. Fletcher et al. (2009) suggests a number of different ways to use an approximate fourth-order dispersion relation to derive coupled partial differential equations (PDEs). When the combination of Thomsen parameters (Thomsen, 1986)  $\epsilon - \delta$  is either

positive or negative a different PDE is necessary.

To avoid shear-wave artifacts and to avoid solving a coupled system of PDEs Etgen and Brandsberg-Dahl (2009) suggested the pseudo-analytic method that, instead of solving a coupled system of PDEs, solves a second-order PDE but with spatial derivatives defined by pseudo-differential operators. The method of Etgen and Brandsberg-Dahl (2009) interpolates between exact solutions. However it does not handle variable tilt angle in TTI media. Song and Fomel (2010) split the pseudo-analytical propagator into two parts using a Fourier finite difference approximation.

We first review the derivation of the dispersion relation for anisotropic media. Second, we discuss pseudo-acoustic wavefield propagation in isotropic media (Wards et al., 2008b; Etgen and Brandsberg-Dahl, 2009). We then show how to use a dispersion relation in a rotated coordinate system. Finally, we discuss wavefield propagation in anisotropic media. We use wavefield propagation in anisotropic heterogeneous media to migrate a number of synthetic seismic datasets using a reverse-time migration.

## DISPERSION RELATIONS FOR P AND S WAVES IN ANISOTROPIC MEDIA

Waves in the earth can be modeled using the elastic wave equation. This assumes that the earth is a lossless linear elastic solid where inertia terms are ignored. The elastic stiffness matrix  $c_{ijkl}$  contains 21-independent quantities. We may further simplify the physics by assuming that the elastic stiffness matrix has TTI symmetry. This reduces the number of independent quantities to 7, 2 orientation angles and 5 elastic constants.

Pseudo-acoustic wave equations are simplifications of the elastic-wave equation that only propagate a single mode without coupling effects. Instead, each mode propagates with the same phase velocity as the corresponding mode determined by the dispersion relation derived from the elastic-wave equation. The linear elastic wave equation is (Aki and Richards, 2002)

$$\rho \frac{\partial^2 U}{\partial t^2} = \tau_{ij,j} = c_{ijkl} U_{k,lj}, \quad (1)$$

where  $U(\vec{x})$  is the particle displacement and  $c_{ijkl}$  is the elastic stiffness tensor relating the components of stress  $\tau_{ij}$  with the components of the strain  $e_{kl}$  via the generalized Hooke's Law

$$\tau_{ij} = c_{ijkl} e_{kl}. \quad (2)$$

The strain tensor is defined in terms of the displacements via the relation,

$$e_{kl} = \frac{1}{2} \left( \frac{\partial U_k}{\partial x_l} - \frac{\partial U_l}{\partial x_k} \right) \quad (3)$$

The Einstein index summation convention is used throughout where repeated indexes are summed over.

A general plane wave can be written in the form

$$U_k = d_k \exp(i\omega(n_l x_l / v - t)), \quad (4)$$

where  $d_k$  is the polarization direction,  $\omega$  is the frequency,  $n_l$  is the unit outward normal. Substituting a plane wave into the equation of motion gives

$$(c_{ijkl}n_jn_l - \rho v^2\delta_{ik}) = 0. \quad (5)$$

Let  $\Gamma_{kl} = c_{ijkl}n_jn_l$  then equation 5 is equivalent to

$$(\Gamma_{kl} - \rho v^2\delta_{ik}) = 0. \quad (6)$$

This is an eigenvalue problem and since  $\Gamma_{kl}$  is positive and symmetric the 3 eigenvalues  $\rho v^2$  are positive and real. The eigenvectors corresponding to each eigenvalue are the polarization vector of the plane waves (e.g., Tsvankin, 2001).

In the case of vertical transverse anisotropy (VTI) the eigenvalues or velocities in Thomsen (1986) anisotropic parameters  $\epsilon$ ,  $\delta$ ,  $\gamma$ ,  $V_{P_0}$ , the vertical P-wave velocity, and velocity  $V_{S_0}$ , the vertical S-wave velocity  $V_{S_0}$  are,

$$V_P(\theta)^2 = V_{P_0}^2 \left[ 1 + \epsilon \sin^2 \theta - \frac{f}{2} + \frac{f}{2} \sqrt{1 + \frac{4 \sin^2 \theta}{f} (2\delta \cos^2 \theta - \epsilon \cos 2\theta) + \frac{4\epsilon^2 \sin^4 \theta}{f^2}} \right] \quad (7)$$

$$V_{SV}(\theta)^2 = V_{P_0}^2 \left[ 1 + \epsilon \sin^2 \theta - \frac{f}{2} - \frac{f}{2} \sqrt{1 + \frac{4 \sin^2 \theta}{f} (2\delta \cos^2 \theta - \epsilon \cos 2\theta) + \frac{4\epsilon^2 \sin^4 \theta}{f^2}} \right] \quad (8)$$

$$V_{SH}(\theta)^2 = V_{S_0}^2 [1 + 2\gamma \sin^2 \theta] \quad (9)$$

where  $f = 1 - V_{S_0}/V_{P_0}$  and  $V_{S_0}$  is the vertical S-wave velocity and  $V_{P_0}$  is the vertical P-wave velocity.

Equations (7), (8), and (9) can be linearized about the small parameters  $\epsilon$ ,  $\delta$ , and  $\gamma$  to give,

$$V_P(\theta)^2 = V_{P_0}^2 [1 + (2\delta - 2\epsilon) \sin^2 \theta \cos^2 \theta + 2\epsilon \sin^2 \theta], \quad (10)$$

,

$$V_S V(\theta)^2 = V_{S_0}^2 \left[ 1 + \frac{V_{P_0}^2}{V_{S_0}^2} (2\epsilon - 2\delta) \sin^2 \theta \cos^2 \theta \right], \quad (11)$$

,

$$V_{SH}(\theta)^2 = V_{S_0}^2 [1 + 2\gamma \sin^2 \theta]. \quad (12)$$

This linearization is designed for NMO correction of seismic data and so is less accurate for velocities near horizontal propagation. For other possible approximations of the dispersion relation see Fowler (2003).

## WAVENUMBER REPRESENTATION OF DISPERSION RELATIONS

The dependence of the wavefield on the direction of propagation is achieved through expressing the dispersion relation in terms of wavenumbers,  $\vec{k}$ . In terms of the dip  $\theta$

$$\begin{aligned} k_x &= |\vec{k}| \sin \theta \\ k_z &= |\vec{k}| \cos \theta, \end{aligned} \quad (13)$$

in 2D, and in terms of the azimuth  $\alpha$ ,

$$\begin{aligned} k_x &= |\vec{k}| \sin \theta \cos \phi \\ k_y &= |\vec{k}| \sin \theta \sin \phi \\ k_z &= |\vec{k}| \cos \theta, \end{aligned} \quad (14)$$

in 3D. Substituting equation (13) into equation (8) gives a dispersion relation,

$$\omega_{V_{SV}}^2(k_x, k_z)^2 = |\vec{k}|^2 V_{P_0}^2 \left[ 1 + \epsilon \sin^2 \theta - \frac{f}{2} - \frac{f}{2} \sqrt{1 + \frac{4 \sin^2 \theta}{f} (2\delta \cos^2 \theta - \epsilon \cos 2\theta) + \frac{4\epsilon^2 \sin^4 \theta}{f^2}} \right],$$

or in terms of  $k_x, k_z$  the dispersion relation is

$$\omega_{V_{SV}}^2(k_x, k_z) = V_{P_0}^2 \left[ k^2 \left(1 - \frac{f}{2}\right) + \epsilon k_x^2 - \frac{f}{2} \sqrt{k^4 + \frac{4k_x^2}{f} (2\delta k_z^2 - \epsilon(k_z^2 - k_x^2)) + \frac{4\epsilon^2 k_x^4}{f^2}} \right]. \quad (15)$$

For TTI media the axis of rotation is not aligned with the coordinate axis. Given a tilt of angle  $\beta$  from vertical, the dispersion relation for the weak linearly approximation is

$$V_P^2(\theta)^2 = V_{P_0}^2 [1 + (2\delta - 2\epsilon) \sin^2(\theta - \beta) \cos^2(\theta - \beta) + 2\epsilon \sin^2(\theta - \beta)]. \quad (16)$$

We would like to express the dispersion relation in terms of  $\beta, k_x$ , and  $k_z$  because the angle  $\beta$  is spatially dependent. In terms of a rotation matrix  $R(\beta)$  the dispersion relation is

$$\omega_{R(\beta)}(\vec{k}, \vec{x}) = \omega(R(\beta)\vec{k}, \vec{x}) \quad (17)$$

In general, the angle  $\beta$  will be spatially dependent.

## WAVEFIELD PROPAGATION IN ISOTROPIC HOMOGENEOUS MEDIA

The following conventions are used for the forward and inverse Fourier transform of the function  $\varphi : \mathbb{R}^3 \rightarrow \mathbb{C}$ ,

$$\hat{\varphi}(\vec{k}) = \mathcal{F}_{\vec{x} \rightarrow \vec{k}}(\varphi) = \int_{\mathbb{R}^3} e^{2\pi i \vec{x} \cdot \vec{k}} \varphi(\vec{x}) dx dy dz, \quad (18)$$

and

$$\varphi(\vec{x}) = \mathcal{F}_{\vec{k} \rightarrow \vec{x}}^{-1}(\hat{\varphi}) = \int_{\mathbb{R}^3} e^{-2\pi i \vec{x} \cdot \vec{k}} \hat{\varphi}(\vec{k}) dk_x dk_y dk_z, \quad (19)$$

where  $\mathbb{R}$  is the real line,  $i = \sqrt{-1}$ ,  $\vec{x} = (x, y, z) \in \mathbb{R}^3$ ,  $\vec{k} = (k_x, k_y, k_z) \in \mathbb{R}^3$  is the Fourier domain coordinate conjugate to  $\vec{x}$ , and the hat denotes a Fourier transformed function of the spatial coordinates. The symbols  $\mathcal{F}_{\vec{x} \rightarrow \vec{k}}$ , and  $\mathcal{F}_{\vec{k} \rightarrow \vec{x}}^{-1}$  are used to denote the forward and inverse Fourier transforms as abstract operators, respectively. Later, the symbols  $\mathcal{F}_{\vec{x} \rightarrow \vec{k}}$ , and  $\mathcal{F}_{\vec{k} \rightarrow \vec{x}}^{-1}$  are also used to denote the Fourier-like integrals when  $\varphi$  or  $\hat{\varphi}$  depending upon both  $\vec{k}$  and  $\vec{x}$  explicitly. In this case, a single FFT cannot be used to calculate the Fourier transform.

Common wave-equation depth migration methods recursively extrapolate the recorded wavefield downward in depth. In contrast, RTM, like forward modelling, recursively propagates the recorded wavefield in time. This is typically done by finite-differencing the two-way wave equation. As an alternative to finite-differencing the wave equation, our time-stepping equation is formulated by phase-shifting the Fourier transform of the wavefield with a cosine operator (Wards et al., 2008a). The time-stepping equation is based on an exact solution of the constant-velocity acoustic-wave equation,

$$\frac{\partial^2 U}{\partial t^2} = v^2 \left( \frac{\partial^2 U}{\partial x^2} + \frac{\partial^2 U}{\partial y^2} + \frac{\partial^2 U}{\partial z^2} \right), \quad (20)$$

where  $U(t, \vec{x})$  is the amplitude of the wave at the point  $(t, \vec{x} = (x, y, z))$ ,  $x, y$  are the lateral coordinate,  $z$  is the depth coordinate,  $t$  is the time coordinate,  $\partial^2 U / \partial t^2$  is, for example, the second-order partial derivative of the wavefield with respect to the time coordinate, and  $v$ , a constant, is the speed of propagation.

Assume  $\vec{x} \in \mathbb{R}^3$  and  $t \in \mathbb{R}$ . Applying the Fourier transform over the spatial dimensions  $\vec{x} = (x, y, z)$  to both sides of equation (20) reduces it to a collection of ordinary differential equations,

$$\frac{\partial^2 \hat{U}}{\partial t^2} = -(2\pi)^2 v^2 (k_x^2 + k_y^2 + k_z^2) \hat{U}. \quad (21)$$

Given the initial conditions,

$$\begin{cases} U(0, \vec{x}) = f(\vec{x}) \\ U(-\delta t, \vec{x}) = g(\vec{x}) \end{cases}, \quad (22)$$

where  $\delta t$  denotes a timestep, the exact solution at time  $t = \delta t$  of constant velocity wave equation is

$$U(\delta t, \vec{x}) = -U(-\delta t, \vec{x}) + 2\mathcal{F}_{\vec{k} \rightarrow \vec{x}}^{-1}[\cos(2\pi v |\vec{k}| \delta t) \mathcal{F}_{\vec{x} \rightarrow \vec{k}}[U(0, \vec{x})]]. \quad (23)$$

The solution can be calculated by iterating equation (23). The calculation at time step  $n$  corresponding to time  $t = n\delta t$  is expressed as,

$$U^{n+1}(\vec{x}) = -U^{n-1}(\vec{x}) + 2\mathcal{F}_{\vec{k} \rightarrow \vec{x}}^{-1}[\cos(2\pi v |\vec{k}| \delta t) \mathcal{F}_{\vec{x} \rightarrow \vec{k}}[U^n(\vec{x})]]. \quad (24)$$

The fast Fourier transform can be employed to compute equation (23) because the kernel of the Fourier integral is independent of the spatial coordinate  $\vec{x}$ .

## WAVEFIELD PROPAGATION IN ISOTROPIC INHOMOGENEOUS MEDIA

The variable-velocity acoustic wave equation is

$$\frac{\partial^2 U}{\partial t^2} = v^2(x, y, z) \left( \frac{\partial^2 U}{\partial x^2} + \frac{\partial^2 U}{\partial y^2} + \frac{\partial^2 U}{\partial z^2} \right), \quad (25)$$

where  $v(x, y, z)$  is the spatially dependent velocity. We now adapt equation (23) which propagates an acoustic wavefield exactly in a constant velocity medium to propagate approximately in a variable velocity medium. Equation (25) has a local causality property which means that the wavefield  $U(t, \vec{x})$  only depends on the wavefield locally. As a result, the right hand side of equation (25),  $v^2(\vec{x}) (U_{xx} + U_{yy} + U_{zz})$ , can, for small enough  $\delta t$ , be approximated locally near  $\vec{x}_0$  by the solution to the frozen term  $v^2(\vec{x}_0) (U_{xx} + U_{yy} + U_{zz})$ . This means that by replacing the constant velocity appearing in the dispersion relation in equation (23) by the variable velocity (i.e. unfreezing the velocity), we have an approximate solution

$$U^{n+1}(\vec{x}) = -U^{n-1}(\vec{x}) + 2\mathcal{F}_{\vec{k} \rightarrow \vec{x}}^{-1} \left[ \cos \left( 2\pi v(\vec{x}) |\vec{k}| \delta t \right) \mathcal{F}_{\vec{x} \rightarrow \vec{k}} [U^n(\vec{x})] \right]. \quad (26)$$

Or explicitly,

$$U^{n+1}(\vec{x}_1) = -U^{n-1}(\vec{x}_1) + 2 \int_{\mathbb{R}^3} \int_{\mathbb{R}^3} U^n(\vec{x}) \cos \left( 2\pi v(\vec{x}_1) |\vec{k}| \delta t \right) e^{2\pi i (\vec{x} - \vec{x}_1) \cdot \vec{k}} dx dy dz dk_x dk_y dk_z. \quad (27)$$

This is the freezing-unfreezing argument that appears in the literature in the context of hyperbolic and elliptic partial differential equations e.g., (p. 230-231, Stein, 1993). Such solutions are often called locally homogeneous approximations (e.g., Ma and Margrave, 2008) and they approximate the solution to the variable velocity wave equation by the solution locally from the constant velocity wave equation. In fact the locally homogeneous approximation is used for both finite-difference and pseudospectral solvers.

A partition of unity is used to partition the velocity model into  $N$  regions with approximate constant velocity,  $v_1 < \dots < v_j < \dots < v_J$ , called reference velocities. In our method these regions can be spatially very complex when the velocity varies rapidly. The wavefield in each region is then propagated with the corresponding reference velocity. The POU is used to window the wavefield into regions at each timestep and the combination of windowing and Fourier transformation results in the Gabor approximation to equation (26) given by

$$U^{n+1}(\vec{x}) = -U^{n-1}(\vec{x}) + \sum_{j=1}^N \Omega_j(\vec{x}) 2\mathcal{F}_{\vec{k} \rightarrow \vec{x}}^{-1} \left[ \cos \left( 2\pi v_j |\vec{k}| \delta t \right) \mathcal{F}_{\vec{x} \rightarrow \vec{k}} [U^n(\vec{x})] \right], \quad (28)$$

where  $v_j$  is the reference velocity used for propagation in the  $j$ th window  $\Omega_j(\vec{x})$  and the integrations are then all FFT's.

The computational burden of the PSTS equation depends linearly on the number of reference velocities used to approximate the the cosine operator. Constructing accurate

approximations with a minimal number of reference velocities allows numerically efficient phase-shift time-stepping algorithms. Methods for choosing reference velocities are found in, for example, Bagaini et al. (1995) or Ma and Margrave (2008). A simple method is to take the reference velocities equally spaced between the lowest and greatest velocity. A spatially discontinuous partition of unity can be used to approximate equation (26). Suppose that a set of reference velocities have been chosen so that  $v_1 < \dots < v_j < \dots < v_J$  where  $v_1$  and  $v_N$  are the minimum velocity and maximum velocity of  $v(\vec{x})$ , respectively. Suppose  $\sum_j \Omega_j(\vec{x})v_j^2 = v^2(\vec{x})$  and  $\sum_j \Omega_j(\vec{x}) = 1$  with  $0 \leq \Omega_j(\vec{x}) \leq 1$ . The auxiliary condition that  $\Omega_j(\vec{x}) = 0$  if  $v(x) > v_{j+1}$  or  $v(x) < v_{j-1}$  so that the operator is interpolated between the closest reference velocities. The  $\Omega_j$ 's window and interpolate the wavefield propagated with constant velocities and form a partition of unity. Then (Etgen and Brandsberg-Dahl, 2009),

$$\Omega_j(\vec{x}) = \begin{cases} \frac{v^2(\vec{x})-v_{j-1}^2}{v_j^2-v_{j-1}^2} & v_{j-1} < v(x) < v_j \\ \frac{v_{j+1}^2-v^2(\vec{x})}{v_{j+1}^2-v_j^2} & \text{if } v_j < v(x) < v_{j+1} \\ 0 & \text{otherwise} \end{cases} \quad (29)$$

To approximate equation (26), we propagate the wavefield with a collection of constant velocities and then recombine the result with the partition of unity,

$$U^{n+1} = \sum_{j=1}^J \Omega_j(\vec{x}) \mathcal{F}_{\vec{k} \rightarrow \vec{x}}^{-1} \left[ 2 \cos(2\pi v_j |\vec{k}|) \mathcal{F}_{\vec{x} \rightarrow \vec{k}} [U^n] \right] - U^{n-1}. \quad (30)$$

Expanding the cosines in equation (30) and (26) with the power series expansion about  $v = 0$  shows that equation (30) is at least as accurate as a second-order pseudospectral method. Choosing the reference velocities and windows as above makes the windowing scheme effectively an interpolation between reference velocities.

## WAVEFIELD PROPAGATION IN ANISOTROPIC HOMOGENEOUS MEDIA

Given a dispersion relation  $\omega(\vec{k})$  we may define a wave equation whose phase velocity is the same as the phase velocity derived from the elastic wave equation for any particular body wave mode. We define a homogeneous anisotropic wave equation with phase velocity  $\omega(\vec{k}, \vec{x})$  as

$$\frac{\partial^2 U}{\partial t^2} = -\mathcal{F}_{\vec{k} \rightarrow \vec{x}}^{-1} \left( \omega^2(\vec{k}) \widehat{U}(\vec{k}) \right). \quad (31)$$

This equation is hyperbolic provided  $\omega(\vec{k}) > 0$ . When  $\omega$  is independent of  $\vec{x}$  equation (31) has the solution

$$U^{n+1}(\vec{x}) = -U^{n-1}(\vec{x}) + 2\mathcal{F}_{\vec{k} \rightarrow \vec{x}}^{-1} \left[ \cos \left( \omega(\vec{k}) \delta t \right) \mathcal{F}_{\vec{x} \rightarrow \vec{k}} [U^n(\vec{x})] \right], \quad (32)$$

for the initial conditions  $U(0, \vec{x}) = U^0$ ,  $U(\delta t, \vec{x}) = U^1$ .

## WAVEFIELD PROPAGATION IN ANISOTROPIC HETEROGENEOUS MEDIA

In the case of variable velocity we may replace the constant dispersion relation with a heterogeneous dispersion relation  $\omega(\vec{k}, \vec{x})$ , Equation (31) has an approximate solution

$$U^{n+1}(\vec{x}) = -U^{n-1}(\vec{x}) + 2\mathcal{F}_{\vec{k} \rightarrow \vec{x}}^{-1} \left[ \cos \left( \omega(\vec{k}, \vec{x}) \delta t \right) \mathcal{F}_{\vec{x} \rightarrow \vec{k}} [U^n(\vec{x})] \right]. \quad (33)$$

Wavefield propagation in heterogeneous anisotropic media can be achieved by approximating equation (33). This is done by approximating the kernel of the Fourier integral operator  $\cos(\omega(\vec{k}, \vec{x})\delta t)$  with a set of functions that are separately a function of  $\vec{x}$  and  $\vec{k}$ , e.g.

$$\cos\left(\omega(\vec{k}, \vec{x})\delta t\right) = \sum_{i=1}^N F_i(\vec{x})G_i(\vec{k}). \quad (34)$$

This allows the computation of equation (33) with a forward Fourier Transform and  $N$  inverse Fourier transforms. One method of calculating is by expanding the cosine in power series expansion about the parameters  $\epsilon, \delta, \gamma, \theta, V_p, \beta,$  and  $V_s$ .

## NUMERICAL EXAMPLES

To demonstrate wavefield propagation with equation (33) a few impulse responses are calculated in homogeneous TTI media. Although both P and SV wave modes are propagated separately both are displayed over top of each other for convenience. Figure 1 is the image of a variety of impulses propagated with pseudo-acoustic wave equations. In the top left of Figure 1 is a pure SV impulse response using the exact dispersion relation. In the top right of Figure 1 is an image of two overlaid impulse responses using the exact P-wave and the exact S-wave dispersion relations. In the bottom left part of Figure 1 is the impulse responses from a linear P-wave dispersion relation and a quadratic linearization of the S-wave dispersion relation. A simple linearization is not sufficiently accurate for S waves. In the bottom right of the figure is the difference between the P-wave and S-wave impulse responses described above. Figure 2 is the exact same as Figure 1 except the value of  $\delta$  is  $-0.2$  instead of being  $0.1$ . For the choice of anisotropic parameters in Figure 2 there is a triplication of the SV wavefronts.

Figure 3 is the vertical P-wave reflectivity for a VTI model made by Hess. The Hess synthetic seismic dataset was generated using a pseudo-acoustic wave equation with a VTI velocity model. The reflection energy in Figure 4 compares to the P-wave reflectivity. There is considerable noise caused by crosscorrelation artifacts.

The ramp model contains three layers with the top layer having a homogeneous TTI velocity. Figure 5 is the vertical velocity. Figure 6 is a migrated image of the vertical component. No attempt was made to separate the P-wave energy from the S-wave energy on the vertical component. The ramp was correctly located.

A simple ray tracing model of a flat reflector in an OBC geometry was created to test PS imaging. Figure 9 (a) displays the ray path of the node gather. The node is located at depth of 1000m, and the shots are located along the sea surface at a depth of 10m. Figure 9 (b) is a node gather for OBC geometry made with ray tracing. Note that in a normal converted wave experiment the zero offset trace would be zero. Figure 9 (c) is migrated image of the PP data for a single shot record. It is correctly imaged. Figure 9 (d) is the migrated image using RTM of the converted wave PS data. The converted wave image is higher frequency than the P-wave image because the shear-wave velocity is half the velocity of the P-wave velocity.

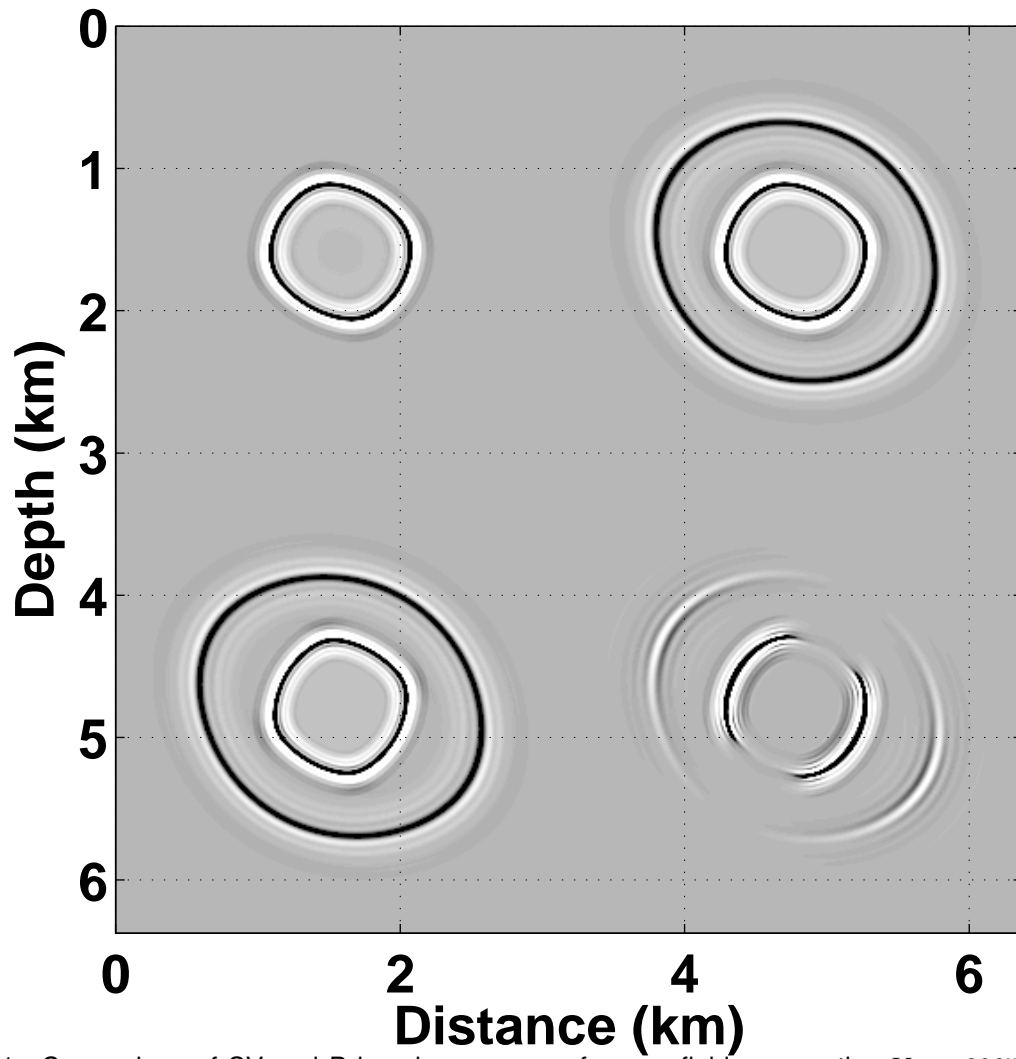


FIG. 1. Comparison of SV and P impulse response for wavefield propagation  $V_p = 2965$ ,  $V_s = 1485$ ,  $\epsilon = 0.196$ ,  $\delta = 0.1$ , and the tilt angle  $\beta = 30^\circ$ . The P and SV waves are propagated separately.

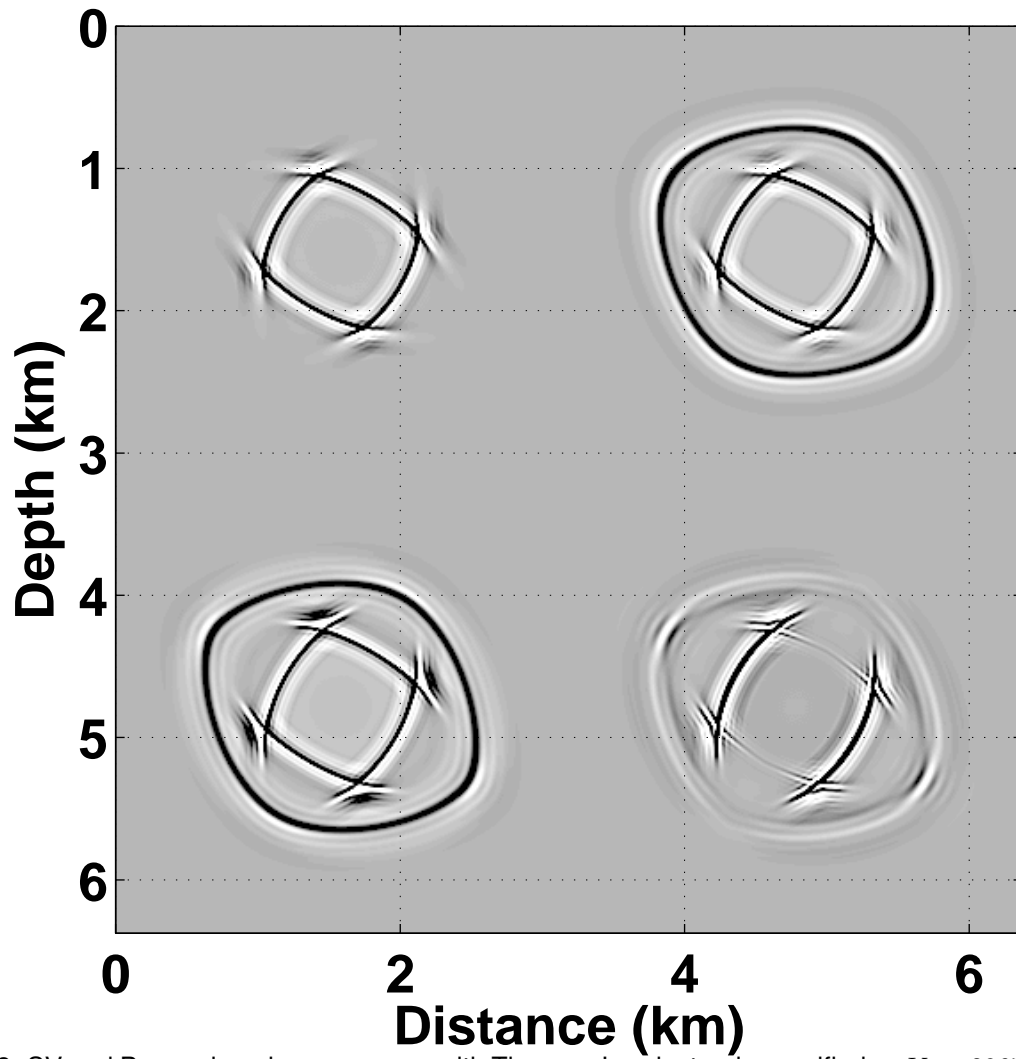


FIG. 2. SV and P wave impulse responses with Thomsen's anisotropic specified as  $V_p = 2965$ ,  $V_s = 1485$ ,  $\epsilon = 0.196$ ,  $\delta = -.2$ , and the tilt angle  $\beta = 30^\circ$ .

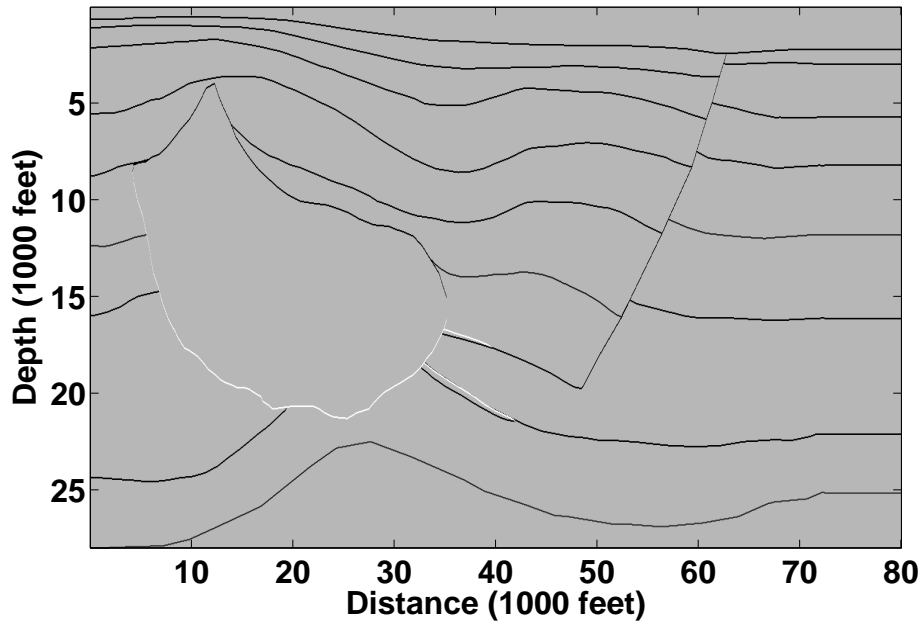


FIG. 3. PP reflectivity for the vertical P-wave velocity. The velocity is expressed in the units  $km/s$ .

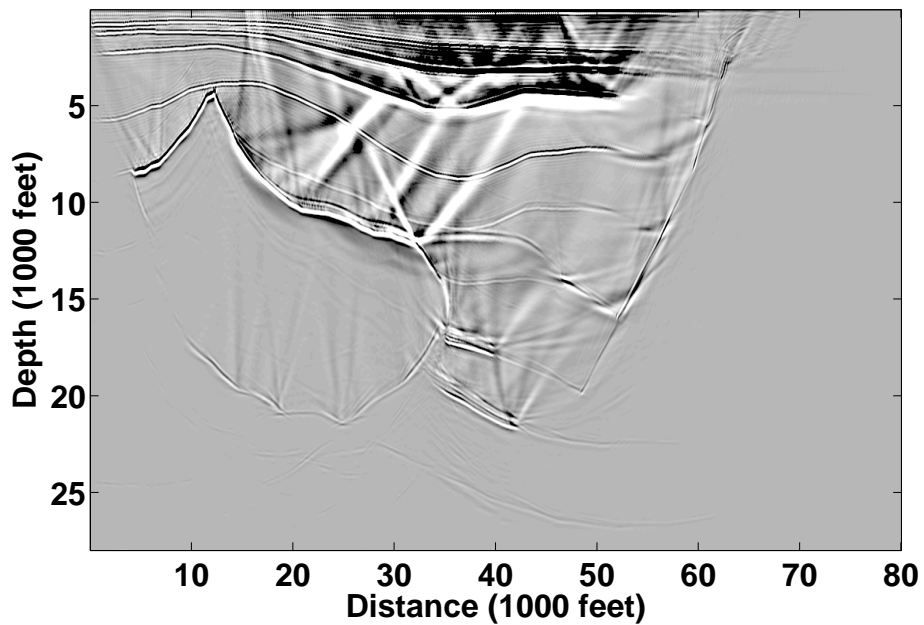


FIG. 4. A migrated image of the Hess VTI data set using a VTI RTM.

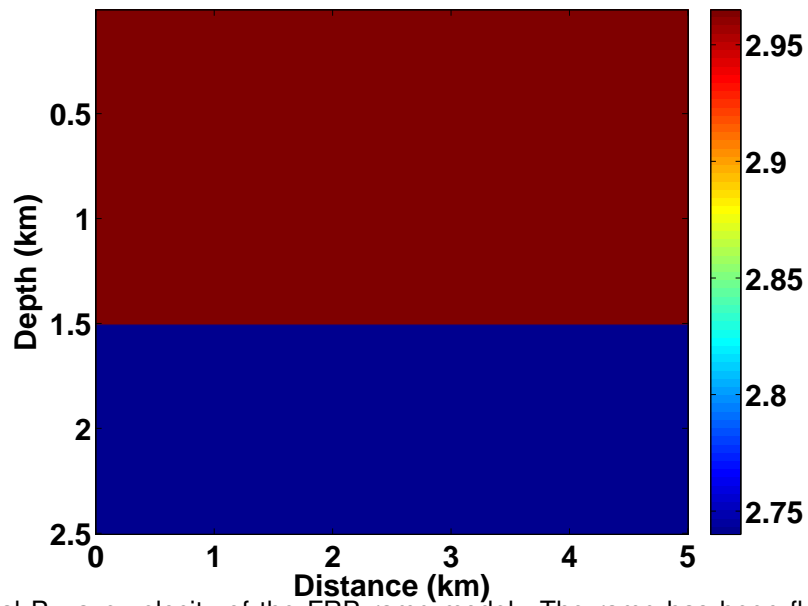


FIG. 5. Vertical P-wave velocity of the FRP ramp model. The ramp has been flooded with the velocity above it. The overburden has a value of  $V_p = \epsilon = 0.196$ ,  $\delta = 0$ , and tilt angle of  $\beta = 45^\circ$ . The lower velocity layer is isotropic.

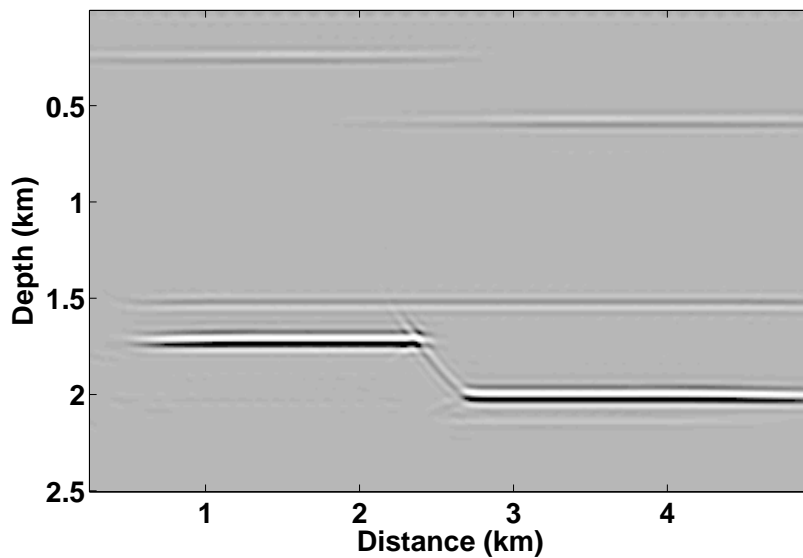


FIG. 6. A PP migrated image of the FRP ramp model which has TTI overburden.

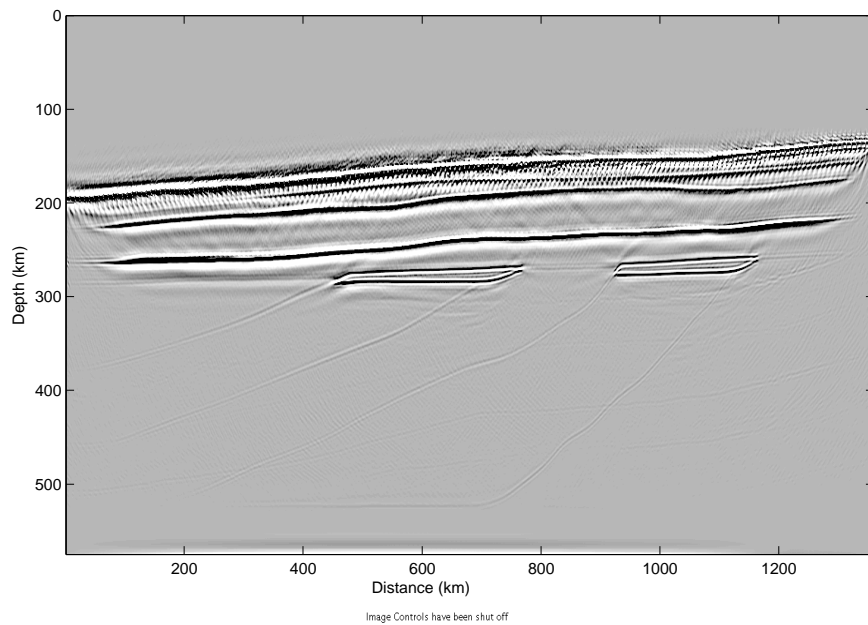


FIG. 7. A migrated image of an ocean bottom cable (OBC) dataset obtained from CCGVeritas. The velocity model is isotropic. The node spacing on the seabed surface is 100m and the shot spacing is 12.5m. The dataset was generated with an elastic wave equation.

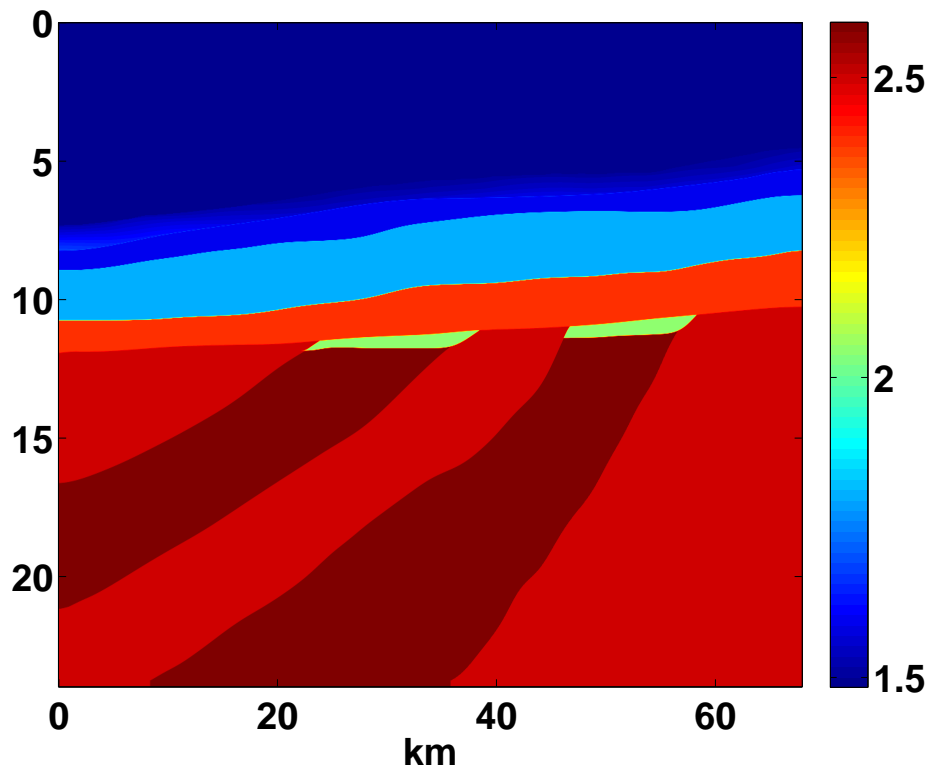


FIG. 8. The P-wave velocity of an OBC dataset provide by CCGVeritas. The units of the velocity are in  $m/s$ .

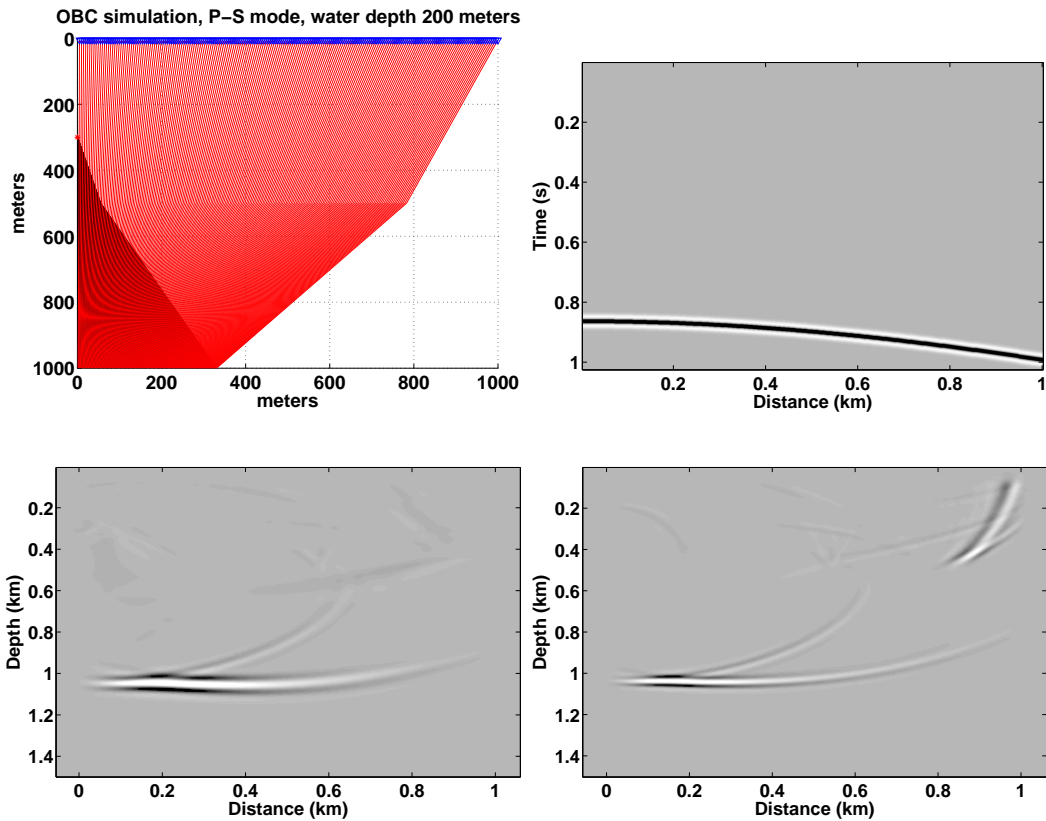


FIG. 9. OBC PP and PS imaging of synthetic data set made with ray tracing. The amplitudes are constant on the reflector. (a) An ocean bottom cable geometry (OBC) with an S-wave source. This is kinematically equivalent to a node gather. (b) PS synthetic data, made with constant amplitude. (c) PP image of a migrated shot made with travel times only. (d) PS image of a migrated shot made with travel times only.

## CONCLUSION

Pseudo-acoustic P and S wave propagators derived from the elastic-wave equation can be used for reverse-time migration. They offer considerable computational advantage over propagating the full elastic wavefield. A second-order pseudo-differential equation is preferred to propagating with a coupled system of partial differential equation that has shear-wave artifacts and instability issues. The derived pseudo-acoustic wave equations were used to migrate a number of synthetic datasets. They provided accurate imaging of reflection data.

## ACKNOWLEDGEMENTS

We thank the Hess Corporation for making the Hess VTI dataset publicly available and CCGVeritas for providing the OBC dataset and for the MITACS internship under which some of this research was conducted. We thank Richard Bale for sharing his insightful knowledge of converted waves and ocean bottom cable surveys. Additionally, we thank the sponsors of the CREWES project, and those of the POTSI consortium, and especially NSERC, MITACS, PIMS, and Alberta Ingenuity.

## REFERENCES

- Aki, K., and Richards, P., 2002, *Quantitative Seismology*: University Science Books.
- Alkhalifah, T., 2000, An acoustic wave equation for anisotropic media: *Geophysics*, **65**, No. 4.
- Bagaini, C., Bonomi, E., and Pieroni, E., 1995, Data parallel implementation of 3-D PSPI: 65nd Ann. Internat.Mtg., Soc. Expl. Geophys., Expanded Abstracts,, **188-191**.
- Etgen, J. T., and Brandsberg-Dahl, S., 2009, The pseudo-analytical method: Application of pseudo-Laplacians to acoustic and acoustic anisotropic wave propagation: SEG Technical Program Expanded Abstracts, **28**, No. 1.
- Fletcher, R. P., Du, X., and Fowler, P. J., 2009, Reverse time migration in tilted transversely isotropic (TTI) media: *Geophysics*, **74**, No. 6.
- Fowler, P., 2003, Practical VTI approximations: a systematic anatomy: *Journal of Applied Geophysics*, **54**, No. 3-4.
- Grechka, V., Zhang, L., and III, J. W. R., 2004, Shear waves in acoustic anisotropic media: *Geophysics*, **69**, No. 2.
- Ma, Y., and Margrave, G. F., 2008, Seismic depth imaging with the Gabor transform: *Geophysics*, **73**, No. 3.
- Song, X., and Fomel, S., 2010, Fourier finite-difference wave propagation: SEG Technical Program Expanded Abstracts, **29**, No. 1, 3204–3209.
- Stein, E., 1993, *Harmonic analysis : real-variable methods, orthogonality, and oscillatory integrals*: Princeton University Press.

- Thomsen, L., 1986, Weak elastic anisotropy: *Geophysics*, **51**, No. 10, 1954–1966.
- Tsvankin, I., 2001, *Seismic signatures and analysis of reflection data in anisotropic media*: Elsevier.
- Wards, B. D., Margrave, G. F., and Lamoureaux, M. P., 2008a, Phase-shift time-stepping for reverse-time migration: *SEG Technical Program Expanded Abstracts*, **27**, No. 1.
- Wards, B. D., Margrave, G. F., and Lamoureaux, M. P., 2008b, Phase-shift time-stepping for reverse-time migration: the Marmousi data experience: *CREWES Research Report*.